Journal of Hazardous Materials 362 (2019) 358–367

Contents lists available at ScienceDirect

Journal of Hazardous Materials

journal homepage: www.elsevier.com/locate/jhazmat

Arsenite and chromate sequestration onto ferrihydrite, siderite and goethite nanostructured minerals: Isotherms from flow-through reactor experiments and XAS measurements

S. Hajji[a,*], G. Montes-Hernandez[b,*], G. Sarret[b], A. Tordo[b], G. Morin[c], G. Ona-Nguema[c], S. Bureau[b], T. Turki[a], N. Mzoughi[d]

[a] Natural Water Treatment Laboratory, Water Researches and Technologies Center (CERTE), Technopark of Borj-Cedria, PO Box 273, Soliman, 8020, Tunisia
[b] University Grenoble Alpes, CNRS, ISTerre, CS 40700, F-38058, Grenoble Cedex 9, France
[c] IMPMC, CNRS-Paris6-UPMC, F-75252, Paris, France
[d] High Institute of Sciences and Technology of Environment of Borj Cedria, University of Carthage, Tunisia

GRAPHICAL ABSTRACT

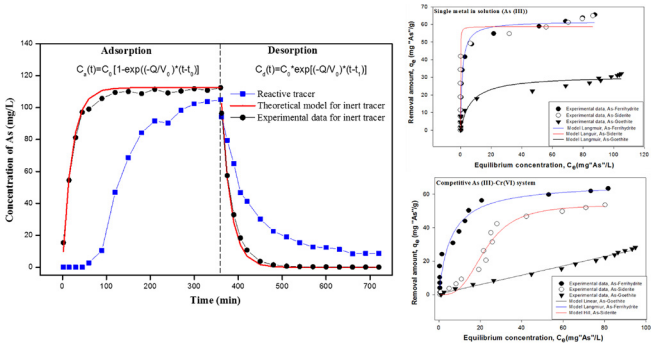

ARTICLE INFO

Keywords:
Water treatment
Heavy metals
Sorption isotherms
Nanostructured iron minerals
Flow-through reactor

ABSTRACT

Sorption isotherms remain a major tool to describe and predict the mobility of pollutants in natural and anthropogenic environments, but they are typically determined by independent batch experiments. In the present study, the sequestration of As(III), Cr(VI) and competitive As(III)-Cr(VI) on/in 6L-ferrihydrite, siderite and goethite nanostructured minerals was reinvestigated using stirred flow-through reactor experiments. Herein, sorption isotherms were particularly determined from breakthrough curves for inert and reactive tracers monitored simultaneously in a single percolation experiment. In complement, X-ray absorption spectroscopy (XAS) was used to identify As sorption sites on 6L-ferrihydrite and goethite. As expected, the minerals have high potential to remove As and Cr from water (siderite = ferrihydrite (about 60 mg/g) > goethite (20 mg/g)). As and Cr sorption isotherms were modelled with a Langmuir model, and with a sigmoidal Hill model in the case of the competitive sorption. XAS measurements have revealed that As(III) was partially oxidized (up to 22%) in the competitive system with chromate oxyanion Cr(VI). As(III) sorbed on ferrihydrite and goethite adopted edge-sharing and corner sharing complex geometries. Nowadays, a new class of adsorbing phases is being developed

* Corresponding authors.
E-mail addresses: sabahhaj@gmail.com (S. Hajji), german.montes-hernandez@univ-grenoble-alpes.fr (G. Montes-Hernandez).

https://doi.org/10.1016/j.jhazmat.2018.09.031
Received 23 June 2018; Received in revised form 1 September 2018; Accepted 11 September 2018
Available online 14 September 2018
0304-3894/ © 2018 Published by Elsevier B.V.

for wastewater treatment, including engineered nanostructured materials and nanocomposites. The use of flow through reactor experiments as a high throughput method, combined with XAS, should be considered as efficient screening methods to test their sorbing properties on various contaminants.

1. Introduction

Heavy metals and metalloids are often released into the environment as a result of industrial activities such as microelectronics, electroplating, metal finishing, battery manufacture, tannery, metallurgical, fertilizer industries. Toxic ions can be transferred into the human and other life organisms via inhalation, ingestion, and skin adsorption, causing irreversible disruptions [1]. They are not biodegradable and, hence, may cause long-term contamination of aquatic ecosystems [2]. In this way, the development of efficient techniques for the removal As, Cr, Se and several other toxic ions from water and wastewater is an important task in terms of protection of public health and environment. These techniques need to take into account the chemical speciation of metal(loid)s. For example, arsenic is commonly present in two valence states: arsenite As(III) and arsenate As(V) [3]. Arsenic (III) is considered to be 25–60 times more toxic than As(V) and more mobile in the environment [4], so potentially more difficult to remove from wastewater. On the other hand, chromium is one of most toxic metals from the hazardous heavy metals list. Similarly to As, it can exist in a different oxidation states, with the trivalent Cr(III) and hexavalent Cr(VI) state being relatively stable and largely predominant [5]. Contrary to arsenic, trivalent chromium is approximately 300 times less toxic than the hexavalent chromium form [5]. Obviously, these two dangerous toxic ions can coexist in various anthropogenic systems due to water pollution by heavy metals [6–14]. In practice, several simple and sophisticated methods are available to remove these toxic ions from wastewater, such as chemical precipitation [6], ion exchange [7], membrane filtration [8], electrocoagulation [9], phytoremediation [10], oxidation-reduction processes, reverse osmosis, chemical coagulation followed by filtration and adsorption [11]. Among these methods, the sorption by using non expensive solid-adsorbents remains efficient and its functioning and technological requirements are also simpler [12,7–14]. For example, significant advantages of the adsorption method are high efficiency in removing very low levels of heavy metals from dilute solutions, easy handling, high selectivity, lower operating cost, minimization of chemical or biological sludge, and in some cases the adsorbent can be regenerated or simplify confined in controlled disposal systems [15]. Extensive research has been performed on the removal of toxic ions from wastewater by sorption processes, i.e. by using simple adsorbent-solution interactions in batch stirred reactors (independent experiments) and this quantified in terms of the “sorption isotherms”. Back in the 1990′s, more sophisticated method by using stirred flow-through reactors was proposed to determine the sorption isotherms [16,17] and it offers a more realistic interpretation linking the kinetic to equilibrium behavior for a well-defined adsorbent-solution system in percolation mode; unfortunately, this efficient method was not popularized and rare studies are found in the literature. Besides, in the last three decades, several studies were oriented to determine the fixation mechanism of ions and/or pollutants onto/into solid phases at the atomic scale by using synchrotron-based X-ray absorption spectroscopy (XAS) [18]. Obviously, such studies have significantly contributed to existing knowledge on the sorption and/or sequestration mechanism of toxic ions at the mineral-solution interfaces. Nevertheless, the “sorption/sequestration isotherms”, a curve describing the retention of pollutants on a solid at various concentrations, remain a major tool to describe and predict their mobility in natural and anthropogenic environments. In this way, the sequestration of As and Cr in/on some iron minerals (6L-ferrihydrite, goethite and siderite) freshly synthesized (using house lab-methods) was re-investigated by using the stirred flow-through reactor experiments. These minerals were selected because they are widespread in soils and drinking aquifers. On the other hand, arsenite and chromate oxyanions were selected because they are toxic natural or anthropogenic ions than can imply redox reactions at the solution-mineral interfaces. Herein, the experimental isotherms for As and Cr were determined from a integrating method using experimental breakthrough curves for inert and reactive tracers and then correctly fitted by using conventional empirical models (Langmuir and sigmoidal Hill models). In complement, some solid samples were characterized by XAS in order to determine the fixation mechanism and oxidation state of As and Cr.

2. Materials and methods

2.1. Synthetic minerals and solutions

In this experimental study, powdered and high-purity nanostructured minerals were used in order to track the As (III) or Cr (VI) trapping onto/into solid phase surfaces. A brief description of these mineral syntheses is provided in the following paragraphs. The physicochemical properties (e.g., particle size, morphology and surface area) of the three synthesized iron oxides have been summarized in a Table 1.

2.1.1. Siderite

Siderite spherical mesocrystals ($FeCO_3$), i.e. micrometer-size spherical aggregates composed by oriented crystalline siderite nanoparticles (size < 100 nm) were synthesized at room temperature by using a multi-step method recently described in Montes-Hernandez and Renard [19]. Briefly, high-carbonate alkaline solution (1 M HCO_3^-) prepared by carbonation of NaOH solution was directly reacted with $FeCl_2$ salt in a controlled reactor and the siderite formation was monitored in real-time by Raman spectroscopy. The solid phase was recovered by simple centrifugation and washed one time with ultrapure water. Then, the particles were washed twice with ethanol and dried at 40 °C for 24 h.

2.1.2. Ferrihydrite

Siderite mesocrystals synthesized at room temperature (see above) were recovered by centrifugation and washed one time with ultrapure water. The wet particles were then dried under air conditions at 60 °C during 24 h. This simple drying process led to a simultaneous de-carbonation of siderite particles and iron oxidation from Fe(II) to Fe(III). In

Table 1
Morphology and average of siderite, ferrihydrite and goethite particles measured from FESEM observations.

The synthesized iron oxides	Morphology	FESEM				N_2 sorption isotherms
		L: length (nm)	W: width (nm)	L/W ratio	Particle size (nm)	S_{BET} (m^2/g)
Ferrihydrite	Spherical mesocrystals	–	–	–	< 20	204
Siderite	Spherical mesocrystals	–	–	–	< 40	90
Goethite	Low acicular	250 ± 35	65 ± 20	3.8	–	133.8

Table 2
Characteristics of Grenoble drinking water used in this study.

Parameter	Value	Quality limit (Order of 11 January 2007)	Quality Reference (Order of 11 January 2007)
pH (at 239 °C)	7,7	–	[6,5–9]
Conductivity (μS cm^{-1}) (at 25 °C)	431	–	[200–1100]
Total organic carbon (mg L^{-1})	< 030	–	2
Total hardness (°F)	21,2	–	–
Chlorides (mg L^{-1})	8,0	–	250
Nitrates (NO_3) (mg L^{-1})	3,6	50	–
Nitrites (NO_2) (mg L^{-1})	< 0,02	0,5	–
Sulfates (mg L^{-1})	46	–	250
Complete alkalimetric title (°F)	158	–	–

such simple conditions, 6L-ferrihydrite (porous aggregates conserving the siderite mesocrystals morphology with high specific surface area, 204 m^2/g) were then synthesized (see Fig. SI1).

2.1.3. Goethite

Low acicular goethite (α-FeOOH) with a high specific surface area (133.8 m^2/g) was synthesized by placing 1 moL of NaOH and 0.2 moL of $FeCl_3.6H_2O$ in a 2 L reaction cell and adding 1 L of high-purity water. Constant agitation (400 rpm) of the solution and a moderate temperature (30 °C) for 24 h of reaction was maintained. For more specific details on the synthesis procedure and goethite characterization refer to Montes-Hernandez et al. [20].

2.1.4. As- and cr-containing solutions

1 L of Grenoble drinking water was used to prepare synthetic solutions enriched with single or/and double metal ions by using commercial salts of As(III) and Cr(VI). A brief description of characterization of Grenoble drinking water is provided in the following Table 2. For more specific details on the characterization of Grenoble drinking water, we can find the monthly analyzes in the town of Saint Martin d'Heres, "swimming pool" area. Grenoble drinking water was preferred rather high-purity or demineralized water because it is more representative of freshwater aquifer. Herein, 200 mg of $AsNaO_2$ (sodium arsenic supplied by Sigma–Aldrich) was used for the As(III) solution (As concentration 115 mg L^{-1}) and 38 mg of K_2CrO_4 (potassium chromate provided by Sigma–Aldrich) for the Cr(VI) solution (Cr concentration 10.2 mg L^{-1}). Solutions containing simultaneously the two pollutants were also prepared to investigate on the competitive sequestration.

2.2. Stirred flow-through reactor experiments

To track the As (III), Cr (VI) or simultaneous As-Cr trapping on/in nanostructured minerals, two stirred flow-through reactors were used (see Fig. SI2). Herein, two flow-through reactors of 50 mL (internal volume) were firstly filled with Grenoble drinking water, one reactor containing 1 g of synthetic mineral (ferrihydrite, goethite or siderite) (reactive tracer reactor). The reactor without mineral-adsorbent was used as inert tracer reference (inert tracer reactor). Moreover, this latter reactor enables to asses if the ionic pollutant is sequestered on the walls (reactor and plastic-tubes) during percolation. Then, flow rate calibration and washing during 10–20 minutes using a peristaltic pump, an As-rich, Cr-rich or As-Cr-rich solution was simultaneously percolated in both reactors using a constant flow rate of 2.3 mL/min. The mineral-solution suspension in the reactor was continuously stirred by a magnetic Teflon bar at room temperature (20 °C). The outflow solutions were filtered in-situ through 0.2 μm pore size Teflon membranes (located on the top of reactors). The filtered solutions at various times of the experiment were then analyzed by ICP-AES (Inductively Coupled Plasma Atomic Emission Spectrometry, Agilent 720 ES) and their pH was measured. Thereby iron, arsenic and chromium concentrations were measured as a function of time from 2 to 360 min. After 6 h of polluted-solution percolation (adsorption step), the system was stopped except the agitation and the morning after desorption step was started at the same flow rate for about 6 h using Grenoble drinking water. Adsorption and desorption steps using flow-through reactors in our study are summarized by respective breakthrough curves for inert and reactive tracers in the Fig. 1.

Finally, after desorption step, the reactor containing the mineral-

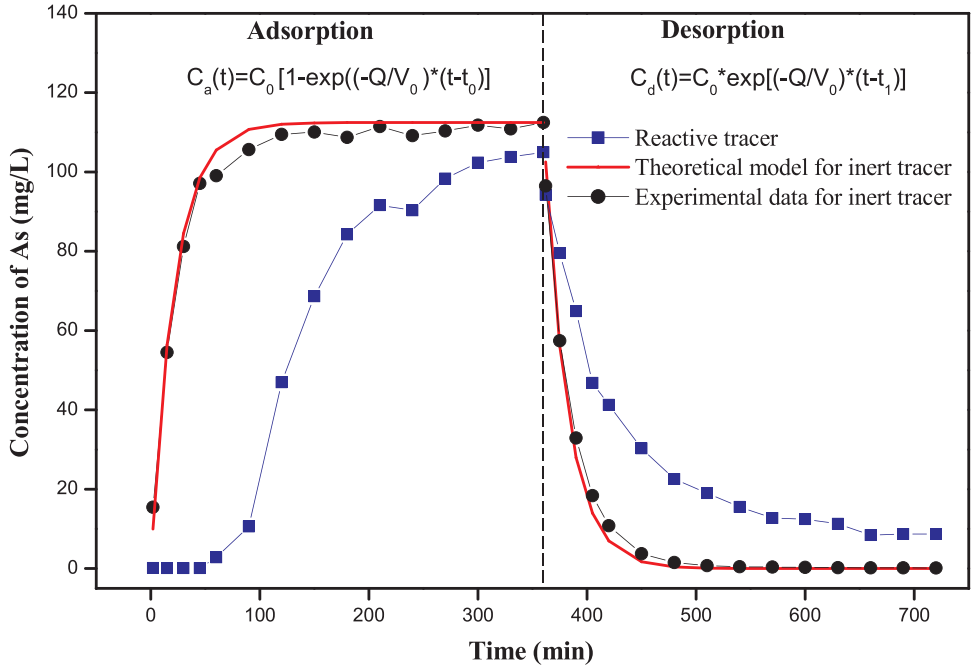

Fig. 1. Experimental sorption and desorption kinetics of inert tracer measured in stirred flow through reactor and comparison between the experiment and theoretical inert tracer. The theoretical BTC is calculated with the reactor volume (V_0) and the flow rate (Q) as Eqs. (1) and (2).

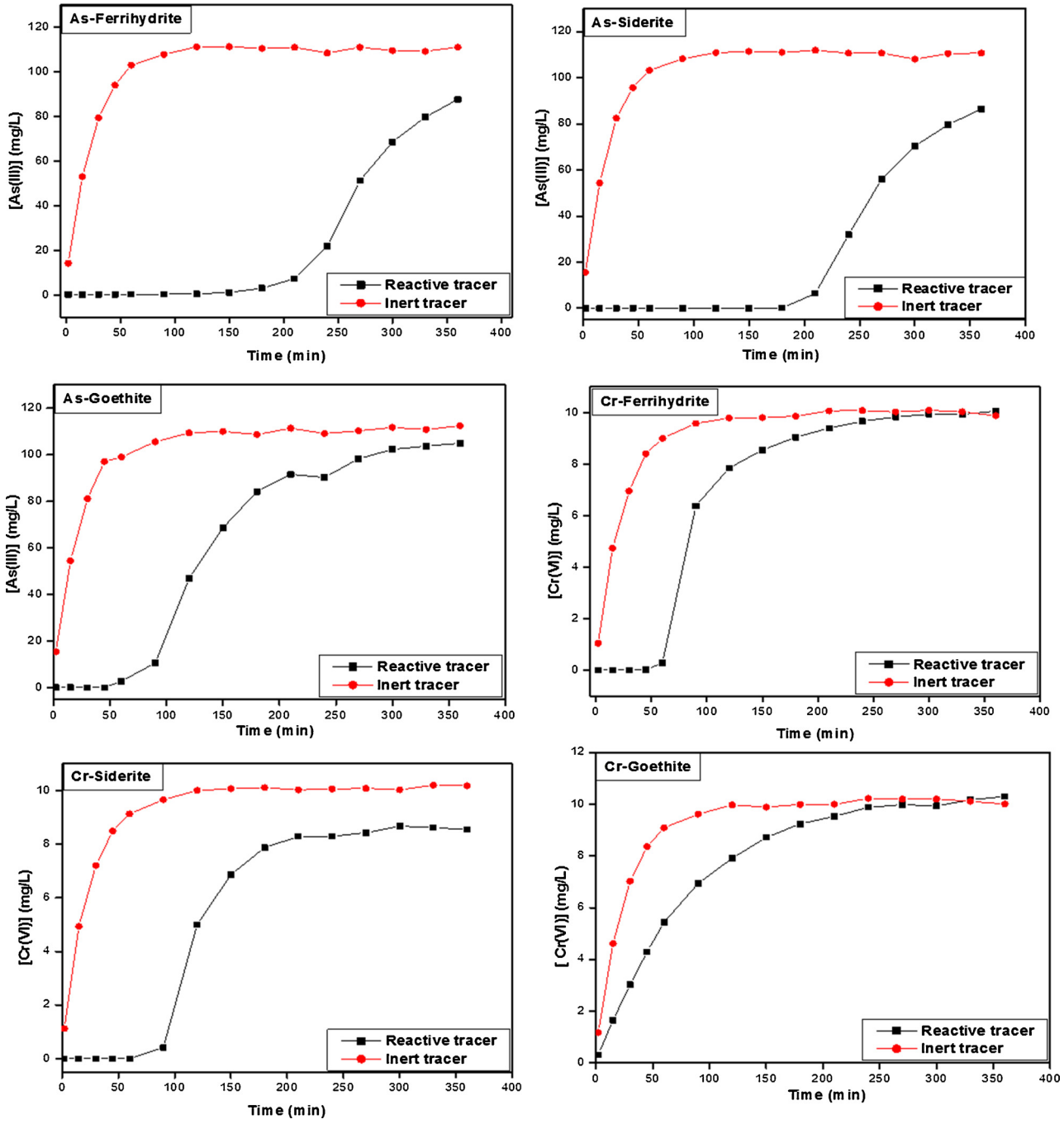

Fig. 2. Results of stirred flow-through reactor experiments: Kinetic adsorption behavior of a single metal(loid) ion on ferrihydrite, siderite and goethite. In all experiments, a similar initial ions concentration about 115 ppm for As(III) and 10 ppm for Cr(VI) were used.

adsorbent was carefully disassembled and the interacting mineral containing As, Cr or both was recovered for future XAS measurements (see below).

2.3. XAS measurements

The list of samples studied by XAS is given in Table SI1. XAS measurements were carried out at the European Synchrotron Radiation Facility (ESRF, Grenoble, France), operating with a ring current of 160–200 mA. Arsenic K-edge XANES and EXAFS spectra were collected on the BM30B (FAME) beamline using a Si(220) double crystal monochromator. The photon flux was of the order of 10^{12} pH s-1. The spectra were collected in fluorescence mode with a 30-element solid-state germanium detector (Canberra), at 15°K using a He cryostat, both as wet paste and after freeze drying. Two to four scans of 40 min each were acquired, and then averaged. Energy calibration was done by recording the spectrum of an Au metallic foil simultaneously to each measurement, and setting the inflection point at 11.919 keV. The oxidation state of As was determined by linear least-squares fitting of XANES data, using linear combinations of XANES spectra of pure As

Table 3
Kinetic parameters from a sigmoidal model [$f = \frac{a}{1+exp(-\frac{x-x_0}{b})}$; Where f: The concentration of the metal in the reactive tracer (mg/L); x: The time (min); a: The maximum concentration of metal; b: The slope of the curve; x_0: The time at which the maximum concentration reaches half].

Mineral	a (mg/L)	b	x_0 (min)
Single metal in solution As(III)			
Ferrihydrite	87.16 ± 1.46	24.31 ± 1.28	264.67 ± 1.62
Siderite	83.83 ± 1.88	22.59 ± 1.84	254.89 ± 2.25
Goethite	99.25 ± 2.03	24.79 ± 2.88	129.87 ± 3.47
Single metal in solution Cr(VI)			
Ferrihydrite	9.39 ± 0.19	9.45 ± 2.56	84.08 ± 2.66
Siderite	8.37 ± 0.14	14.32 ± 2.13	118.17 ± 2.29
Goethite	9.76 ± 0.18	32.57 ± 3.51	59.71 ± 3.69
Competitive As(III)-Cr (VI) system : (fit on the As(III) data)			
Ferrihydrite	103.20 ± 14.69	37.17 ± 6.73	303.42 ± 13.76
Siderite	–	–	–
Goethite	89.30 ± 2.12	38.03 ± 3.85	100.01 ± 4.93

(III)-sorbed ferrihydrite and pure As(V)-sorbed ferrihydrite, as described previously [21]. The uncertainty on the percentages was estimated to ± 2%. Shell fitting of EXAFS spectra was realized as described previously [22].

2.4. Isotherms determination from flow-through reactors

Continuous flow-through reactors are particularly useful for studying mineral–water reaction kinetics [23–25]. It consists in injecting a step of the reactive tracer through a stirred cell containing a known mass of the solid in contact with the solution, and then comparing the breakthrough curves of the reactive solute with that of an inert tracer. In a perfectly stirred flow-through reactor, the solution composition is homogeneous within the reactor and equal to that measured in the outlet flow. The breakthrough curve (BTC) of an inert tracer following a step injection from C = 0 to C_0, is given by Eq. (1) [26].

$$C(t) = C_0\left[1-\exp\left(-\frac{Q}{V_0}(t-t_0)\right)\right] \quad (1)$$

Where t_0 is the instant when the tracer is injected, Q(mL/min) represents the flow rate and V_0 (L) is the volume of the solution inside the reactor (i.e. the volume of the reactor minus the volume of the solid). The ratio Q/V_0 defines the mean residence time in the reactor for an inert tracer. For the desorption stage (switching back the injected concentration to zero), the breakthrough curve of an inert tracer is given by Eq. (2) [26].

$$C(t) = C_0\exp\left(-\frac{Q}{V_0}(t-t_1)\right) \quad (2)$$

Where t_1 is the instant when the injection of the tracer is stopped.

These two fundamental equations can be systematically used as references when reactive tracers are used. In our case, two independent reactors were used to compare simultaneously inert and reactive tracers in the same percolation system (see Fig. 1). This allows a real experimental comparison between reactive and inert tracers. Fig. 1 summarizes clearly the breakthrough curves for arsenic as inert and reactive (goethite as adsorbent) tracers. These experimental curves are then used to determine the adsorption/sequestration isotherm for a given pollutant as follows:

The corresponding adsorbed fraction between C = 0 and C_i is calculated using the integrated area between the breakthrough curves of the inert and reactive tracers inside of a given interval (Fig. 1). Each of these calculations provides one point (C_i, q_i) of the isotherm; assuming an equilibrium concentration in each point as clearly explained by Limousin et al. [26]. The relation to determine the adsorbed/sequestered amount (q_i) for a given equilibrium concentration (C_i) from breakthrough curves can be expressed as:

$$q_i = \frac{\text{Flow rate}}{\text{Solid mass}}A_i = \frac{\text{Flow rate}}{\text{Solid mass}}\left(\int_{t=0}^{t=t_i} C_{\text{inert tracer}}\,dt - \int_{t=0}^{t=t_i} C_{\text{reactive compound}}\,dt\right) \quad (3)$$

The main advantage of this method is that only one percolation experiment is required to determine one isotherm for a given pollutant and probably these continuous flow systems are more reliable to pollutants transfer in natural systems.

3. Results and discussion

3.1. Kinetic behavior: breakthrough curves from stirred flow-through experiments

From experimental breakthrough curves for inert and reactive tracers displayed in Fig. 2 can be noted that the three synthesized adsorbents (ferrihydrite, siderite and goethite) are performants to remove As and Cr from water. In general, a sigmoidal kinetic behavior was observed, this means that during a given period-time the injected pollutant (contained in inlet flow) is rapidly and quasi-totally sequestered onto/into the interacting mineral (Fig. 2). For example, the arsenite oxyanion is quasi-completely removed from solution during about 200 min of percolation when ferrihydrite or siderite is used. After this percolation-time, the available sorption sites start to be saturated in the system up to that the As-concentration in the inlet flow is equivalent/equal to As-concentration in outlet flow. In such situation, all available sorption sites onto mineral are theoretically occupied by As species in equilibrium with interacting solution. As above mentioned, the arsenite oxyanion is also strongly sequestered on

goethite mineral, but in this case, the saturation of sorption sites starts after about 50 min of percolation, indicating that goethite is kinetically less performant that the ferrihydrite and siderite at the investigated conditions.

Concerning the chromate oxyanion, the siderite seems to be the more performant adsorbent because the saturation of adsorption sites starts after about 90 min of percolation, followed by ferrihydrite (60 min). Conversely, the saturation of sorption sites on goethite starts immediately after initiated percolation; this is incongruent with high specific surface area for goethite mineral. This means that the goethite performance to remove Cr is not necessary directly proportion to its specific surface area.

Competitive As-Cr systems were also investigated for [As]/[Cr] ratio ≈ 10; for theses specific cases, the kinetic behavior during sequestration process was significantly impacted; in effect, the saturation of sorption sites starts faster with respect to single ion systems (see Fig. SI3). Herein, ferrihydrite and siderite remain the more performant adsorbents with respect to goethite. This most complex kinetic behavior was probably related to an additional redox process; in fact, Cr(VI) was partially reduced to Cr(III) and As(III) was then oxidized to As(V). This electron transfer operates exclusively at the mineral-solution interfaces as already claimed in the literature [27] and as measured by x-ray absorption spectroscopy (XAS) on some recovered solids in our study (see below). All kinetic parameters for reactive tracer curves using a sigmoidal model are summarized in Table 3. Retarding effect could be also determined by comparing breakthrough curves for inert and reactive tracers, but in our study the so-called curves were particularly

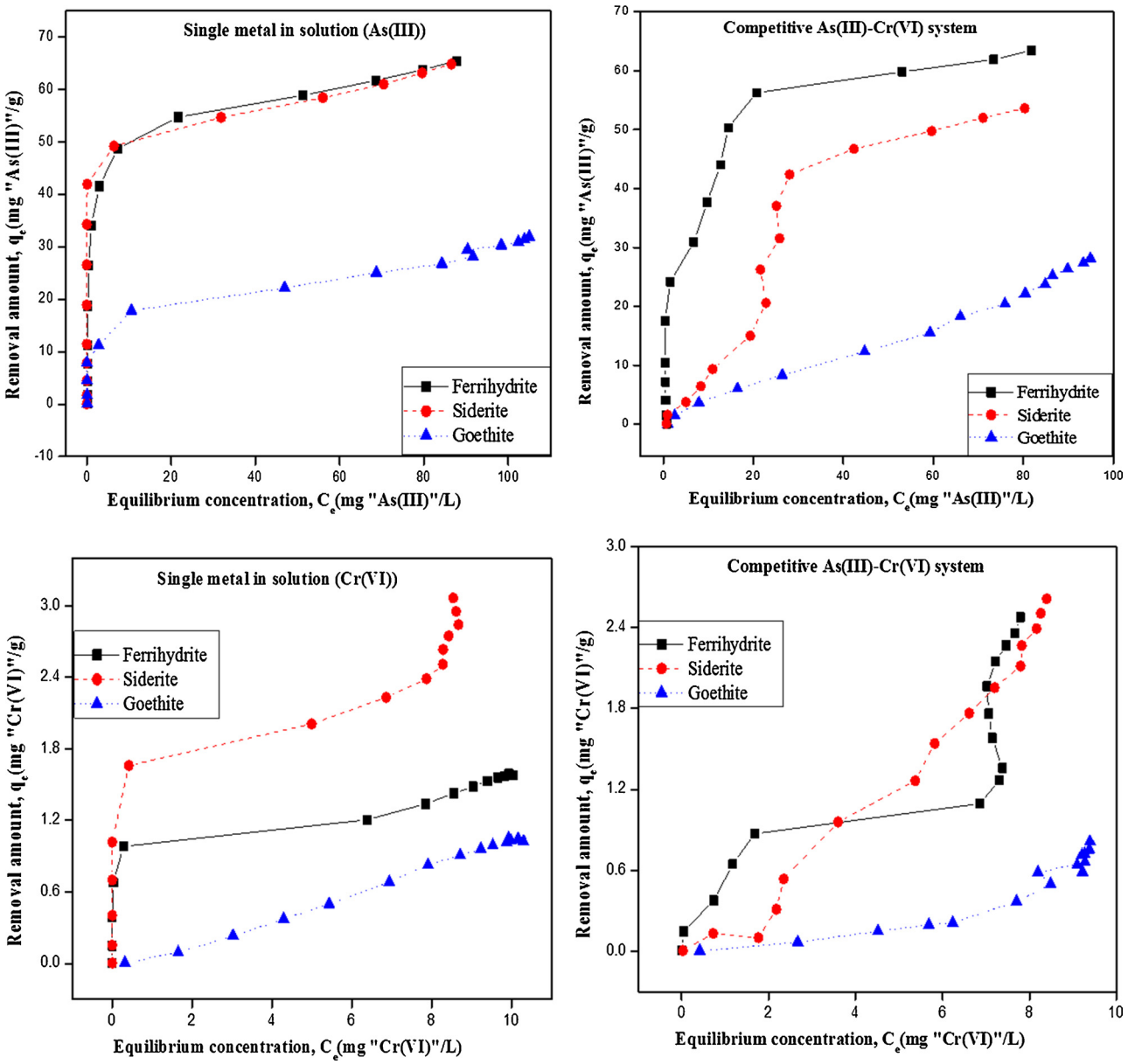

Fig. 3. The adsorption isotherm from the breakthrough curve of an inert and a reactive tracer obtained with the stirred flow-through reactor, assuming that the reaction is instantaneous. The relation between the hatched surface area Ai of the breakthrough curve and the solid concentration Qi is given by $Q_i = \frac{Flow\ rate}{Solid\ mass} A_i = \frac{Flow\ rate}{Solid\ mass} (\int_{t=0}^{t=t_i} C_{inert\ tracer}\ dt - \int_{t=0}^{t=t_i} C_{reactive\ compound}\ dt)$.

used to determine the sorption isotherms (main objective of this study).

As complementary information, the desorption and/or release of sequestered As and Cr was also monitored as illustrated in Fig. 1 by percolating drinking Grenoble water (free of pollutant). As expected, a retarding effect also exists between reactive and inert tracer curves; in fact, 6 h of percolation are not enough to release the sequestered amount of pollutants (see example in Figs. 1 and Fig. SI4); this indicating that the chemisorption process contributes also to the As and Cr sequestration in the investigated iron minerals. Here, the kinetic release follows a hyperbolic decay or kinetic pseudo-second order decay-model while the inter tracer follows a simple exponential decay model (see Fig. 1).

In summary, flow-through reactor experiments offer a direct monitoring of sequestration performance for a given adsorbent comparing the breakthrough curves for inert and reactive tracers. Moreover, theses cited curves enable the determination of sequestration isotherm for an investigated pollutant as discussed in the following paragraphs.

3.2. Isotherms of sorption/sequestration

As explained in material and methods section, the integrated surface comprised between experimental breakthrough curves for inert and reactive tracers allows the determination of sequestration isotherms (see also Eq. 3). In this way, the Fig. 3 summarizes the isotherms obtained for single ions (As and Cr) and competitive As-Cr systems. In general, the isotherms confirm that the three synthesized minerals (ferrihydrite, siderite and goethite) have a high adsorption capacity to remove dissolved As(III) and Cr(VI), oxyanions with very high toxicity in the environment (see introduction section). This is not a surprising result; however, the isotherms for As and Cr reported in literature have

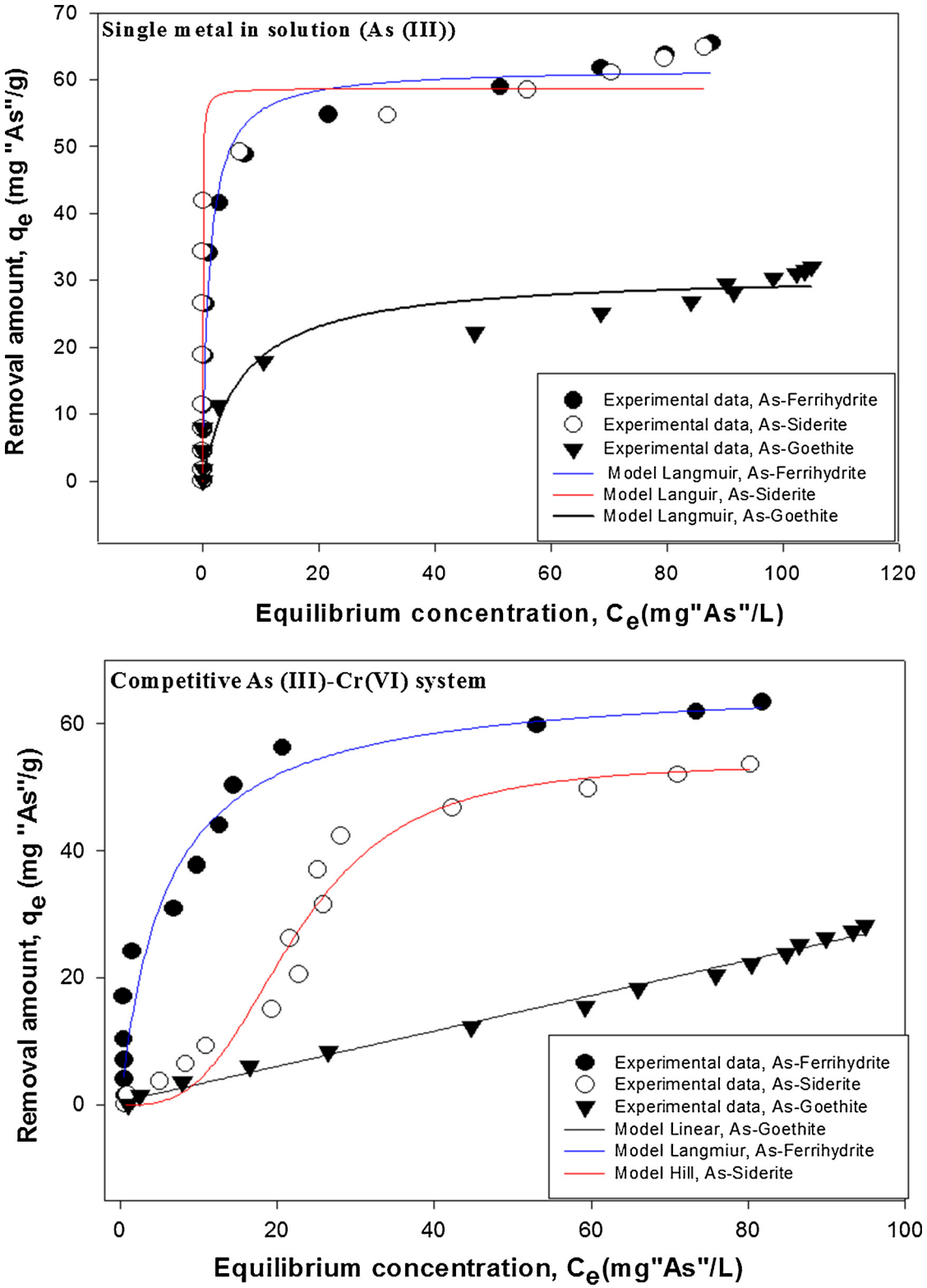

Fig. 4. Modelling of equilibrium isotherms for removal of arsenite from aqueous solutions using three synthetic minerals.

been determined for a smaller concentration range and they were typically obtained from batch independent experiments; in fact, each point in the isotherm represent an independent experiment. Conversely, the flow-through reactor experiments via the experimental breakthrough curves for inert and reactive tracers in our study, have allowed the exploration of all concentration range in a single experiment.

In more specific terms, the siderite and ferrihydrite can sequester up to about 60 mg/g of As(III) in the investigated concentration range (see Fig. 3) and a simple Langmuir model can be used to fit both isotherms (Fig. 4). However, goethite has only sequestered about 20 mg/g of As (III) (Fig. 3), three times less at equivalent specific surface area with respect to siderite; this can be related to a chemisorption processes, but, probably also related to siderite surface oxidation (from Fe(II) to Fe(III) onto the siderite crystals) that can increase the sorption sites. For this

Table 4
Isotherm parameters from conventional Langmuir and sigmoidal Hill models [**Langmuir**: $q_e = \frac{q_{max} K_L C_e}{1 + K_L C_e}$; Where q_e (mg/g) is the amount adsorbed at equilibrium concentration of arsenic or chromium ions in solution C_e, q_{max} (mg/g) is the Langmuir constant representing the maximum adsorption capacity, K_D(L/g) a liquid–solid distribution coefficient. **Hill:** $q_e = \frac{q_{max} C_e^b}{c^b + C_e^b}$; where b is the Hill coefficient, c is the concentration at ½ q_{max}].

Mineral	K_L(L/mg)	q_{max}(mg/g)	K_D(L/g)	R
Single metal in solution As(III)				
Ferrihydrite	0.85	61.79	52.56	0.980
Siderite	0.05	58.74	2.93	0.829
Goethite	0.14	30.96	4.50	0.963
Single metal in solution Cr(VI)				
Ferrihydrite	0.173	66.95	11.60	0.970
Siderite*	0.016*	53.86*	0.86*	0.98*
Goethite	–	–	–	–

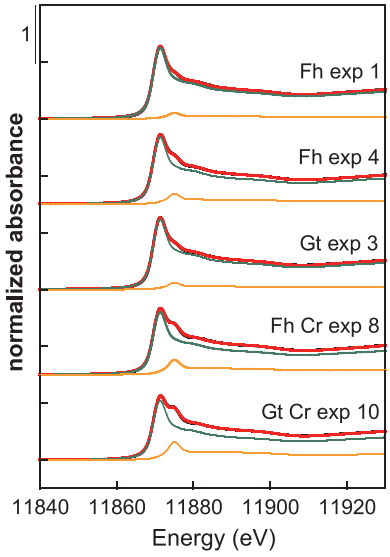

Fig. 5. Linear combination fit of the As K-edge XANES spectra. Experimental and calculated curves are displayed as black and red lines, respectively. The spectra of As(III)- and As(V)-adsorbed ferrihydrite model compounds were used as fitting components with their fitted contributions displayed in green and orange lines respectively (Table 3). (For interpretation of the references to colour in this figure legend, the reader is referred to the web version of this article.)

latter case, Langmuir model was also used to fit the experimental isotherm (see Fig. 4). The isotherms for As(III) in competition with Cr(VI) were strongly affected, mainly when siderite and goethite were used (see Fig. 3). In this case, sequestration isotherm for As using siderite has changed of profile type from Langmuir model (isotherm type L) to sigmoidal Hill model (isotherm type S) (see Fig. 4). This latter is corresponding to a modification of conventional Langmuir model and it is typically used for competitive systems; in our case, the competition is mainly related to redox reactions because the Cr(VI) was partially reduced to Cr(III) and As(III) was oxidized to As(V) as confirmed by XAS measurements (see below). On the other hand, surprising result was measured for the arsenic sorption isotherm when goethite was used; here, isotherm type L was changed to a pseudo-linear behavior (isotherm type C) (see Fig. 4); a redox process could also responsible of this effect. All estimated sorption parameters including liquid–solid distribution coefficients (K_d) for As and Cr by using Langmuir and sigmoidal Hill models are summarized in Table 4. We note that the K_d is the more reliable parameter on the pollutant transfer/mobility through reactive porous media.

Concerning the Cr(VI) sequestration isotherms, the sequestration mechanism seems to be more complex in single and competitive systems (see Fig. 3). In this case, conventional and/or modified Langmuir models seem ineffective to fit obtained experimental isotherms. This is mainly due to concurrent redox reactions during mineral-solution interactions in the investigated systems as clearly attested by XAS measurements.

3.3. XAS determination of the arsenic sequestration mechanism

For the samples without Cr, As K-edge XANES spectra indicated that the wet samples were devoid of As(V) (Fig. SI5A), whereas freeze-drying lead to the oxidation of a small fraction of arsenic, i.e. 7–13 % As (V) over total As, as determined by linear combination fitting (Fig. 5; Table 3). Such minor components are not expected to significantly contribute to the EXAFS [28]. The analysis was then performed on the freeze-dried samples because they had a better signal-to-noise ratio (Fig. SI5B). Shell-by-shell fitting analysis of the EXAFS data evidenced two types of As(III) surface complexes for both ferrihydrite (at the two concentrations tested) and goethite samples: an edge-sharing complex (so-called ^1E, with an As-Fe distance of about 2.9 Å) and a corner sharing complex (so-called ^2C, with an As-Fe distance of 3.3–3.5 Å) (Fig. 6 and Table 5). A similar mixture of ^1E and ^2C sites was found for As(III) sorbed on ferrihydrite, as previously reported in [21,22,29]. At the opposite, only ^2C sites were identified for As(III) sorbed on goethite in previous studies [22,29]. The presence of ^1E As(III) surface complexes on goethite in the present study may be explained by the nano-sized (130 m^2/g) and low-acicular character of the goethite employed in our experiments [19]. Indeed, although ^2C surface complexes are favored on (110 – Pnma *SG*) facets of acicular goethite crystallites, ^1E surface complexes may form on (001) facets [22].

In the presence of Cr, As K-edge XANES spectra for wet samples and freeze dried material were similar (Fig. SI4) and the proportion of As (III) over total As dropped to 83 and 78%, respectively, showing a partial oxidation of As(III) by Cr(VI) at the mineral-solution interfaces. Again, very similar local structures were found for As reacted with ferrihydrite and goethite, with structural parameters typical of As(III) in both ^1E and ^2C geometries. It is not possible from EXAFS to determine whether some Cr has been incorporated in the Fe oxyhydroxide structure and is present in the local environment of As, since Cr and Fe have close atomic numbers ($\Delta Z = 2$) and thus similar backscattering properties.

4. Conclusion

In summary, the stirred flow-through reactor experiments offer a direct monitoring of pollutants sequestration performance for a given adsorbent by comparing the breakthrough curves for inert and reactive tracers. Moreover, the integrated surface comprised between these experimental breakthrough curves (retarding effect) enables the determination of sequestration isotherms for pollutants in a broad concentration range from a single experiment.

On the other hand, novel nanostructured materials (including mineral or organo-mineral phases) for wastewater treatment are under development [30]. Flow through reactors appear as handy and efficient tools for the screening of their efficiency on large series of pollutants and sorbents, and can be considered as high throughput methods. Spectroscopic measurements (XAS, FTIR, XPS, Raman, etc.) are ideal complementary tools to determine the fixation mechanisms of pollutants at the nano- and/or atomic scales.

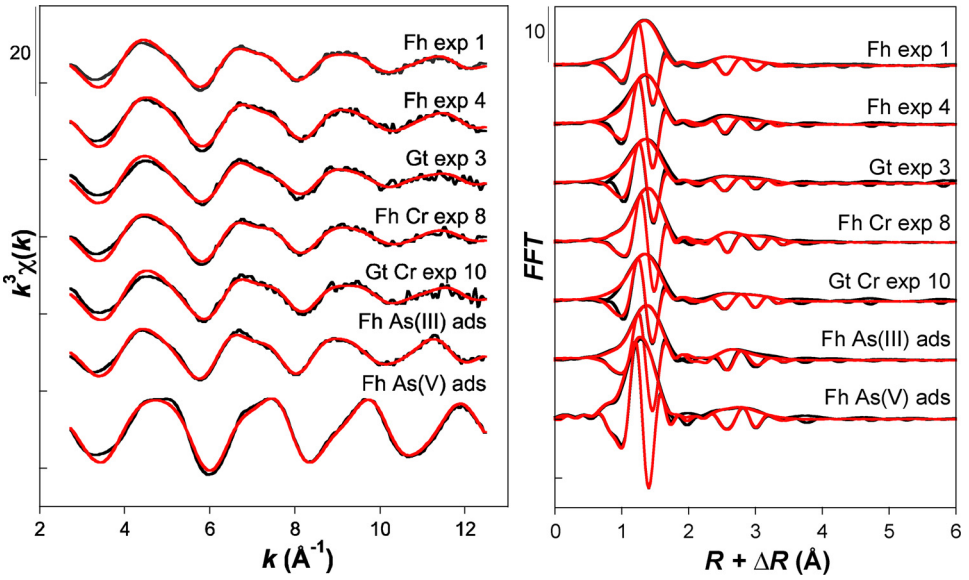

Fig. 6. Unfiltered As K-edge k^3-weighted EXAFS spectra (a) and (b) corresponding Fast Fourier Transforms (FFT) calculated over the 2.5–12.5 *k*-range. Experimental and calculated curves are displayed as black and red lines, respectively. Structural parameters obtained from a shell-by-shell fit of the data in *k*-space are given in Table 3. (For interpretation of the references to colour in this figure legend, the reader is referred to the web version of this article.)

Table 5
Results of XANES linear combination fit and EXAFS shell-by-shell analyses.

	XANES		EXAFS					
Sample	As(III) (%)	As(V) (%)	path	*R* (Å)	*N*	σ(Å)	ΔE_0 (eV)	χ^2_R
Fh Exp 1	94(2)	7(2)	AsO	1.763(5)	3*	0.076(2)	15(1)	16.6
			AsOO	3.1(1)	6*	–	–	
			AsFe	2.92(2)	0.2(1)	0.063(3)	–	
			AsFe	3.38(2)	0.4(2)	–	–	
Fh Exp 4	89(2)	13(2)	AsO	1.754(3)	3*	0.071(2)	16(1)	9.0
			AsOO	3.2(1)	6*	–	–	
			AsFe	2.87(2)	0.3(2)	–	–	
			AsFe	3.34(2)	0.4(1)	–	–	
Gt Exp 3	92(2)	9(2)	AsO	1.761(7)	3*	0.079(3)	16(1)	14.0
			AsOO	3.2(2)	6*	–	–	
			AsFe	2.86(2)	0.3(2)	–	–	
			AsFe	3.33(3)	0.6(3)	–	–	
Fh Cr Exp 8	83(2)	19(2)	AsO	1.749(5)	3*	0.078(2)	15(1)	21.0
			AsOO	3.2(2)	6*	–	–	
			AsFe	2.89(2)	0.6(4)	0.096(3)	–	
			AsFe	3.36(3)	0.6(4)	–	–	
Gt Cr Exp 10	78(2)	23(2)	AsO	1.747(5)	3*	0.076(2)	16(1)	7.0
			AsOO	3.2(2)	6*	–	–	
			AsFe	2.87(3)	0.3(1)	–	–	
			AsFe	3.34(2)	0.6(2)	–	–	
Fh As (III)[a]	100	0	AsO	1.779(3)	3*	0.061(2)	15(1)	16.6
			AsOO	3.2*	6*	–	–	
			AsFe	2.93(1)	0.4(1)	0.061(1)	–	
			AsFe	3.42(2)	0.5(2)	–	–	
Fh As(V) [a]	0	100	AsO	1.687(3)	4*	0.061(2)	5(1)	41.8
			AsOO	3.1(1)	12*	–	–	
			AsFe	3.31(2)	1.0(3)	0.08*	–	

R (Å), interatomic distances; N, number of neighbors;σ(Å), Debye-Waller factor, ΔE_0 (eV), difference between the user-defined threshold energy and the experimentally determined threshold energy in eV. [a] Synthetic model compounds corresponding to As(III) or As(V)-sorbed ferrihydrite previously analyzed by Hohmann et al. (28).

Acknowledgements

The authors are grateful to the French National Center for Scientific Research (CNRS) for providing financial support. Funding from Labex OSUG@2020 (Investissement d'avenir-ANR10-LABX56) is acknowledged. Rodica Chiriac and Nathaniel Findling are thanked for their valuable technical assistance.

Appendix A. Supplementary data

Supplementary material related to this article can be found, in the online version, at doi:https://doi.org/10.1016/j.jhazmat.2018.09.031.

References

[1] J.H. Potgieter, S.S. Potgieter-Vermaak, P.D. Kalibantonga, Heavy metals removal from solution by palygorskite clay, Min.. Eng. 19 (2006) 463–470.
[2] B. Amarasinghe, R.A. Williams, Tea waste as a low cost adsorbent for the removal of Cu and Pb from wastewater, Chem. Eng. J. 32 (2007) 299–309.
[3] D. Mohan, C.U. Pittman, Arsenic removal from water/wastewater using adsorbents—A critical review, J. Hazard. Mater. 142 (2007) 1–53.
[4] P.L. Smedley, D.G. Kinniburgh, A review of the source, behavior and distribution of arsenic in natural waters, App. Geochem. 17 (2002) 517–568.
[5] K.M.S. Sumathi, S. Mahimairaja, R. Naidu, Use of low-cost biological wastes and vermiculite for removal of chromium from tannery effluent, Biores. Technol. 96 (2005) 309–316.
[6] N. Meunier, P. Drogui, C. Montané, R. Hausler, G. Mercier, J.F. Blais, Comparison between electrocoagulation and chemical precipitation for metals removal from acidic soil leachate, J. Hazard. Mater. 137 (2006) 581–590.
[7] S.K. Sahu, P. Meshram, B.D. Pandey, V. Kumara, T.R. Mankhand, Removal of chromium (III) by cation exchange resin, indion 790 for tannery waste treatment, Hydrometallurgy 99 (2009) 170–174.
[8] P. Religa, A. Kowalik, P. Gierycz, A new approach to chromium concentration from salt mixture solution using nanofiltration, Sep. Purif. Technol. 82 (2011) 114–120.
[9] A.K. Golder, A.N. Samanta, S. Ray, Removal of trivalent chromium by electrocoagulation, Sep. Purif. Technol. 53 (2007) 33–41.
[10] L. Mandi, S. Tiglyene, A. Jaouad, Depuration of tannery effluent by phytoremediation and infiltration percolation under arid climate, Options Méditerranéennes 88 (2009) 199–205.
[11] Z. Li, R. Beachner, Z. McManama, H. Hanlie, Sorption of arsenic by surfactant-modified zeolite and kaolinite, Micropor. Mesopor. Mat. 105 (2007) 291–297.
[12] A. Nilchi, S.R. Garmarodi, S.J. Darzi, Removal of arsenic from aqueous solutions by an adsorption process with titania–silica binary oxide nanoparticle loaded polyacrylonitrile polymer, J. Appl. Polym. Sci. 119 (2011) 3495–3503.
[13] H. Aydın, Y. Bulut, C. Yerlikaya, Removal of copper (II) from aqueous solution by adsorption onto low-cost adsorbents, J. Environ. Manage. 87 (2008) 37–45.
[14] M. Eloussaief, M. Benzina, Efficiency of natural and acid-activated clays in the removal of Pb(II) from aqueous solutions, J. Hazard. Mater. 178 (2010) 753–757.
[15] N. Ahalya, T.V. Ramachandra, R.D. Kanamadi, Biosorption of heavy metals, Res. J. Chem. Environ. 7 (2003) 71–78.
[16] D. Grolimund, M. Borkovec, P. Federer, H. Sticher, Measurement of sorption isotherms with flow-through reactors, Environ. Sci. Technol. 29 (1995) 2317–2321.
[17] A. Martin-Garin, P. Van Cappellen, L. Charlet, Aqueous cadmium uptake by calcite: a stirred flow-through reactor study, Geochim. Cosmochim. Acta. 67 (2003) 2763–2774.
[18] G.E. Brown Jr, N.C. Sturchio, An overview of synchrotron radiation applications to low temperature geochemistry and environmental science, Rev. Mineral. Geochem. 49 (2002) 1–115.
[19] G. Montes-Hernandez, F. Renard, Time-resolved in situ raman spectroscopy of the nucleation and growth of siderite, magnesite and calcite and their precursors, Cryst. Growth Des. 16 (2016) 7218–7230.
[20] G. Montes-Hernandez, P. Beck, F. Renard, E. Quirico, B. Lanson, R. Chiriac,

N. Findling, Fast precipitation of acicular goethite from ferric hydroxide gel under moderate temperature (30 and 70 C degrees), Cryst. Growth Des. 11 (2011) 2264–2272.
[21] G. Ona-Nguema, G. Morin, Y.H. Wang, A.L. Foster, F. Juillot, G. Calas, G.E. Brown, XANES evidence for rapid arsenic(III) oxidation at magnetite and ferrihydrite surfaces by dissolved O_2 via Fe^{2+}-mediated reactions, Environ. Sci. Technol. 44 (14) (2010) 5416–5422.
[22] G. Ona-Nguema, G. Morin, F. Juillot, G. Calas, G.E. Brown, EXAFS analysis of arsenite adsorption onto two-line ferrihydrite, hematite, goethite, and lepidocrocite, Environ. Sci. Technol. 39 (23) (2005) 9147–9155.
[23] K.L. Nagy, A.C. Lasaga, Dissolution and precipitation kinetics of gibbsite at 80°C and pH 3: the dependence on solution saturation rate, Geochim. Cosmochim. Acta 56 (1992) 3093–3111.
[24] P. Van Cappellen, L. Qiu, Biogenic silica dissolution in sediments of the Southern Ocean. II. Kinetics, Deep. Sea. Res. Part II. Top. Stud. Oceanogr. 44 (1997) 1129–1149.
[25] J. Villermaux, Génie de la Réaction Chimique : Conception et Fonctionnement des Réacteurs, 2éme edit., Tec et Doc, Paris, France, 1985.
[26] G. Limousin, J.P. Gaudet, L. Charlet, S. Szenknect, V. Barthes, M. Krimissa, Sorption isotherms: a review on physical bases, modeling and measurement, Appl. Geochem. 22 (2007) 249–275.
[27] O.W. Duchworth, S. Martin, Role of molecular oxygen in the dissolution of siderite and rhodochrosite, Geochim. Cosmochim. Acta. 68 (2004) 607–621.
[28] C. Hohmann, G. Morin, G. Ona-Nguema, J.M. Guigner, G.E. Brown Jr, A. Kappler, Molecular-level modes of As binding to Fe(III) (oxyhydr)oxides precipitated by the anaerobic nitrate-reducing Fe(II)-oxidizing *acidovorax* sp. Strain BoFeN1, Geochim. Cosmochim. Acta. 75 (2011) 4699–4712.
[29] B. Cancès, F. Juillot, G. Morin, V. Laperche, L. Alvarez, O. Proux, J.-L. Hazemann, G.E. Brown Jr, G. Calas, XAS evidence of As (v) association with iron oxyhydroxides in a contaminated soil at a former arsenical pesticide processing plant, Environ. Sci. Technol. 39 (2005) 9398–9405.
[30] X. Qu, P.J.J. Alvarez, Q. Li, Applications of nanotechnology in water and wastewater treatment, Water Res. 47 (2013) 3931–3946.